

## General Disclaimer

### One or more of the Following Statements may affect this Document

- This document has been reproduced from the best copy furnished by the organizational source. It is being released in the interest of making available as much information as possible.
- This document may contain data, which exceeds the sheet parameters. It was furnished in this condition by the organizational source and is the best copy available.
- This document may contain tone-on-tone or color graphs, charts and/or pictures, which have been reproduced in black and white.
- This document is paginated as submitted by the original source.
- Portions of this document are not fully legible due to the historical nature of some of the material. However, it is the best reproduction available from the original submission.

NASA Technical Memorandum 7920'

(NASA-TM-79207) STATE-OF-THE-ART OF SIALON  
MATERIALS (NASA) 22 p HC A02/MF A01  
CSCL 11G

N79-30378

Unclas  
G3/27 31865

STATE-OF-THE-ART OF  
SIALON MATERIALS

Sunil Dutta  
Lewis Research Center  
Cleveland, Ohio



Prepared for the  
Forty-ninth Meeting of the Structures and Materials Panel  
including a Specialist Meeting on Ceramics for  
Turbine Engine Applications  
sponsored by AGARD  
Cologne, Germany, October 7-12, 1979

STATE-OF-THE-ART OF SiALON MATERIALS

ORIGINAL PAGE IS  
OF POOR QUALITY

by  
Sunil Dutta  
NASA-Lewis Research Center  
21000 Brookpark Road  
Cleveland, Ohio 44135

SUMMARY

Concurrent with the recent engineering efforts in developing advanced ceramics such as Si<sub>3</sub>N<sub>4</sub> and SiC for structural components of high temperature heat engines, "SiALON" ceramics have also become candidates for consideration. The acronym "SiALON" was originally given to new compositions derived from silicon nitrides and oxynitrides by simultaneous replacement of silicon and nitrogen by aluminum and oxygen. Other metal atoms M such as Be, Mg, Li, and Ga can be incorporated, and the term has become a generic one applied to Si<sub>3</sub>N<sub>4</sub> based materials. In this review, the state-of-the-art of "SiALONs" is examined. The review includes work on phase relations, crystal structure, synthesis, fabrication, and properties of various SiALONs. The essential features of compositions, fabrication methods, and microstructure are reviewed. High temperature flexure strength, creep, fracture toughness, oxidation, and thermal shock resistance are discussed. These data are compared to those for some currently produced silicon nitride ceramics to assess the potential of SiALON materials for use in advanced gas turbine engines.

E-092

INTRODUCTION

Materials currently being evaluated for structural components of high temperature heat engines include Si<sub>3</sub>N<sub>4</sub>, SiC, and a class of materials called SiALONs. The term "SiALON" was adopted to designate any composition containing the elements Si-Al-O-N as major constituents e.g. β'-SiALON (ref. 1,2,3), O'-SiALON (ref. 4), 15R-SiALON (ref. 4) etc. However, most frequently, the term SiALON refers to β-Si<sub>3</sub>N<sub>4</sub> solid solution called β'-SiALON. SiALON compounds can be made by a high temperature reaction between silicon nitride or oxynitride and alumina in which simultaneous replacement of silicon and nitrogen by aluminum and oxygen occurs. Other metal atoms M such as Be, Mg, Li (ref. 5) and Ga (ref. 6) can also be incorporated and the term has thus become a generic one applied to Si-M-O-N based materials. Among various SiALON materials, β'-SiALON has been of great interest because it was claimed to have a low thermal expansion (ref. 2,6), good high temperature modulus of rupture and good oxidation resistance (ref. 7). It was also reported that the β'-SiALON could be fabricated to high density by conventional sintering techniques (ref. 2). These reported properties indicate that β'-SiALON ceramics might be candidates for high temperature applications, and therefore, have generated considerable interest. In this paper, the state-of-the-art of SiALON is examined. The paper reviews work on phase equilibria, structure, fabrication and properties. Based on this review, the potential of SiALON materials for use in advanced gas turbines will be examined.

PHASE EQUILIBRIA AND STRUCTURE

The existence of β'-SiALON in the system Si<sub>3</sub>N<sub>4</sub> - Al<sub>2</sub>O<sub>3</sub> was first reported by Oyama and Kemigaito (ref. 1) in Japan and by Jack and Wilson (ref. 2) in England. Subsequent studies by the same workers reported a solid solution (β'-SiALON) forming region in the systems Si<sub>3</sub>N<sub>4</sub> - SiO<sub>2</sub> - Al<sub>2</sub>O<sub>3</sub> (ref. 5) and Si<sub>3</sub>N<sub>4</sub> - AlN - Al<sub>2</sub>O<sub>3</sub> (ref. 3). Detailed compatibility and phase equilibria studies were reported by Gauckler et. al (ref. 8) and Jack (ref. 4) in the system Si<sub>3</sub>N<sub>4</sub> - AlN - SiO<sub>2</sub> - Al<sub>2</sub>O<sub>3</sub> and their diagrams are shown in Figs. 1 and 2. Jack (ref. 4) refers to his diagram (Fig. 2) as an "Idealized Behavior Diagram" rather than an equilibrium diagram since it combines data obtained from specimens hot pressed at temperatures ranging from 1550 to 2000 C. Most of the data, however, were obtained at 1775 C. On the other hand, the diagram by Gauckler et.al (ref. 8) is an isothermal section at 1760 C (Fig. 1). According to both Jack and Gauckler, the β'-SiALON region extends from the Si<sub>3</sub>N<sub>4</sub> corner in the direction of AlN.Al<sub>2</sub>O<sub>3</sub> along a line representing a constant metal/non-metal (M/X) ratio of 3:4 and can therefore, be described by the empirical formula Si<sub>6-x</sub>Al<sub>x</sub>O<sub>x</sub>N<sub>8-x</sub> with x=0 to 4.2. In the oxygen rich part of the diagram, mullite and X-phase SiALON (formula Si<sub>4</sub>Al<sub>4</sub>O<sub>11</sub>N<sub>2</sub>) were observed. In the AlN-rich part of the system, five new phases were identified (ref. 8) in the region between β'-SiALON and AlN. The phases called X2, X4, X5, X6, and X7 are shown in Fig. 1 and are located along lines of constant metal: non-metal ratios. These were later identified by Jack (Fig. 2) as AlN polytypes (ref.4). The diagrams proposed by Jack and Gauckler et. al. are quite similar except that the locations of AlN polytypes are slightly different. Work by Layden (ref. 9) established the liquidus isotherms (Fig. 3) in part of the system lying between SiO<sub>2</sub>-rich corner of the diagram and X-phase.

β'-SiALON has a β-silicon nitride structure which extends along the 3M/4X line but the sizes of the tetrahedra and hence also the unit-cell dimensions, increase as aluminum and oxygen replace silicon and nitrogen (ref. 8). Silicon oxynitride O'-SiALON

(ref. 4) extends along the 2M/3X (metal/non-metal) line with the  $\text{Si}_2\text{N}_2\text{O}$ -type structure and larger unit-cell dimensions. The structure of X-phase, also designated as "Oyama-Phase" (ref. 4) and "J-phase" (ref. 4) has been interpreted in terms of several different unit cells. Drew and Lewis (ref. 10) proposed a triclinic structure, while Gugel (ref. 11) proposed and orthorhombic lattice. Most recently, the unit cell has been determined to be monoclinic (ref. 4).

Single phase  $\beta'$ -SiAlON forming regions in other systems such as  $\text{Si}_3\text{N}_4 - \text{Al}_2\text{O}_3 - \text{Be}_2\text{SiO}_4$ ,  $\text{Si}_3\text{N}_4 - \text{Al}_2\text{O}_3 - \text{Li}_2\text{O}$  and  $\text{Si}_3\text{N}_4 - \text{Al}_2\text{O}_3 - \text{MgO}$  were reported by Jack (ref. 5), while Oyama (ref. 6) reported a  $\beta'$ -forming region in the system  $\text{Si}_3\text{N}_4 - \text{Al}_2\text{O}_3 - \text{Ga}_2\text{O}_3$ . Extensive ternary solid solutions were found to exist in all of these systems. Detailed phase equilibria in the system  $\text{Si}_3\text{N}_4 - \text{SiO}_2 - \text{Be}_3\text{N}_2 - \text{BeO}$  were reported by Huseby et. al (ref. 12) and are shown in Fig. 4. A large solubility of  $\text{Be}_2\text{SiO}_4$  in  $\beta$ - $\text{Si}_3\text{N}_4$  and of BeO in  $\text{BeSiN}_2$  was found to occur in this system. The solid solubility of  $\text{Be}_2\text{SiO}_4$  in  $\beta$ - $\text{Si}_3\text{N}_4$  decreases with increasing temperature from 19 mol% at 1770 C to 11.5 mol%  $\text{Be}_2\text{SiO}_4$  at 1880 C. There are other single-phase materials in this system and all have moderate solubilities along lines of definite metal:non-metal (M/X) ratios and small solubilities perpendicular to these lines.

In the system  $\text{Si}_3\text{N}_4 - \text{SiO}_2 - \text{AlN} - \text{Al}_2\text{O}_3 - \text{Be}_3\text{N}_2 - \text{BeO}$ , Gauckler (ref. 13) found that the single-phase solid solution with  $\beta$ - $\text{Si}_3\text{N}_4$  structure was restricted to the plane connecting the points  $\text{Si}_3\text{N}_4$ ,  $\text{Be}_2\text{SiO}_4$ ,  $\text{BeAl}_2\text{O}_4$  and  $\text{AlN}:\text{Al}_2\text{O}_3$ . This is shown in Fig. 5a. These four points are co-planar in the quaternary diagram. All composition points on this plane have a constant metal to non-metal ratio of 3:4. The plane of 3:4 is shown in Fig. 5b. A large area of single phase region with the  $\beta$ - $\text{Si}_3\text{N}_4$  structure is located on this plane. No single-phase solid solution was found either above or below this plane.

In the quasiternary system  $\text{Si}_3\text{N}_4 - \text{AlN} - \text{Be}_3\text{N}_2$  shown in Fig. 6, Gauckler et. al (ref. 13) found a complete solid solubility exists from  $\text{AlN}$  to  $\text{BeSiN}_2$ . The lattice parameters in this solid solution with a wurtzite structure increase linearly with increasing Al concentration.

## FABRICATION

### A. Hot Pressing

Hot pressing has been found to be the easiest technique for fabricating theoretically dense, fine-grained bodies with high strength in covalent materials such as  $\text{Si}_3\text{N}_4$  and SiC. Consequently, most early work on phase equilibria, structure, and property evaluation was conducted on  $\beta'$ -SiAlONs fabricated by hot pressing. Table I lists starting materials for various  $\beta'$ -SiAlON formulations and their hot pressing parameters. In most of the investigations, various material combinations listed in Table I were hot pressed at temperatures where simultaneous chemical reaction and densification were taking place under applied pressure. MgO was commonly used as an additive to promote densification. The most effective hot pressing temperature range was 1650-1750 C. Time at temperature varied in these investigations, but generally ranged from approximately 30 minutes to 2 hours. Heating the compacts was accomplished by induction or resistance heating of graphite or SiC. The reaction of carbon with the compact was minimized by using a BN liner or container.

The experimental studies shown in Table I illustrate the varied nature of investigations in hot pressed  $\beta'$ -SiAlONs. Characterization of the hot pressed materials has included phase equilibria, structure, and chemistry which have been discussed in the preceding sections. Strength, creep, thermal and oxidation behavior will be discussed in following sections.

### B. Pressureless Sintering

Pressureless sintering when compared to hot pressing has the advantage of shape capability and high volume production of small as well as large components. The expense of machining prevents hot pressing from being a cost effective process for many applications. As a result, much effort has been devoted to fabrication by pressureless sintering. Table II shows a list of pressureless sintering studies conducted with various material combinations with and without additives. Sintering was conducted at about one atmosphere of nitrogen to produce bodies with densities as high as 98% theoretical. The most effective sintering temperature regime and time period were 1700-1760 C for 2 - 4 hours respectively, although a much broader range of temperature and time was used by different investigators.

Jack (ref. 2) reported that a  $\text{Si}_3\text{N}_4$  and  $\text{Al}_2\text{O}_3$  mixture could be fabricated to dense single phase  $\beta'$ -SiAlON bodies by pressureless sintering. However, other work (ref. 11) indicated that the resulting SiAlON contained other phases. Morgan (ref. 24) predicted in a presentation cited by Layden (ref. 9) that single phase  $\beta'$ -SiAlON compositions having stoichiometries given by the formula  $\text{Si}_{3-x}\text{Al}_x\text{O}_x\text{N}_{4-x}$  would not sinter. Layden (ref. 9) also reported that as a pure phase  $\beta'$ -SiAlON could not be sintered to high final density. However,  $\beta'$  bodies formulated from starting materials that form some liquid at the sintering temperatures could be sintered to high density. For example, Layden introduced the term "transient liquid phase sintering" or TLP. In

this process, SiAlON bodies of composition  $Si_{1.4}Al_{1.6}O_{1.6}N_{2.4}$  were formulated from two prereacted compositions, one of which was X phase which melts in the neighborhood of 1700 C. The second composition was calculated from the lever rule to yield single phase  $\beta'$ -SiAlON when reacted with a predetermined amount of the X-phase at temperatures above 1700 C. The "transient liquid phase sintering" was confirmed by Gauckler et. al (ref. 25) during sintering of  $\beta'$ -SiAlON compositions utilizing as starting materials only AlN and SiO<sub>2</sub> and no additives. Gauckler et. al concluded that different sintering kinetics would be expected for different sets of starting materials e.g. Si<sub>3</sub>N<sub>4</sub>, AlN, SiO<sub>2</sub> powders or Si<sub>3</sub>N<sub>4</sub>, AlN, Al<sub>2</sub>O<sub>3</sub> powders or SiO<sub>2</sub> and AlN powders because of different reaction mechanisms (ref. 25). The formation of liquid facilitates densification and chemical reaction. Drew and Lewis (ref. 10) also observed the formation of liquid phase during sintering of Si<sub>3</sub>N<sub>4</sub> and Al<sub>2</sub>O<sub>3</sub> mixtures.

Recently, Arias (ref. 26) determined the effect of oxygen to nitrogen ratio (O/N) on the pressureless sinterability of SiAlONs of formula  $Si_{2.55}Al_{0.6}O_{\gamma}N_{4-0.66\gamma}$  (where  $\gamma$  varied from 0.57 to 1.92). Utilizing starting materials Si<sub>3</sub>N<sub>4</sub>, AlN, and SiO<sub>2</sub> plus a small amount of Al<sub>2</sub>O<sub>3</sub> from the grinding media but no additive, a maximum density of about 98% of theoretical occurred in the O/N ratio range between 0.2 and 0.3. It is very likely, that liquid formed in various phase fields according to the behavior diagram shown in Fig. 2 and promoted densification in all compositions as  $\gamma$  varied from 0.57 to 1.92.

In contrast to sintering by forming liquid within the system itself, additives which provide a liquid phase at the sintering temperatures are commonly used for densifying Si<sub>3</sub>N<sub>4</sub> based ceramics. For example, Fig. 7 shows typical densification behavior of  $\beta'$ -SiAlON ( $Si_{2.4}Al_{0.8}O_{0.6}N_{3.6}$ ) as a function of temperature (ref. 31). The starting materials used were Si<sub>3</sub>N<sub>4</sub>, AlN, and Al<sub>2</sub>O<sub>3</sub> with 6 and 3 mol% of additives (Y<sub>2</sub>O<sub>3</sub>-SiO<sub>2</sub>). The Y<sub>2</sub>O<sub>3</sub> to SiO<sub>2</sub> molar ratio was constant at 1:2. Sintering was promoted by a liquid formed by an initial reaction between Y<sub>2</sub>O<sub>3</sub>, SiO<sub>2</sub> and Al<sub>2</sub>O<sub>3</sub>. In any case whether a liquid formed by the foreign additives or during sintering of bodies formulated with major constituents such that some liquid is formed at the sintering temperature, a grain boundary glassy phase is retained in the sintered body. It will be seen later that this glassy phase has a controlling influence on the high temperature properties of the sintered body (ref.9).

#### DENSITY AND MICROSTRUCTURE

$\beta'$ -SiAlON compositions have been fabricated to essentially theoretical density by hot pressing, while pressureless sintering has resulted in maximum densities close to 98% of theoretical, (ref. 30, 31). The density values of hot pressed  $\beta'$ -SiAlONs have varied from 3.09 to 3.16 g/cc (ref. 17) depending on the location along the  $\beta'$ -homogeneity line (Fig. 2,3). The density of other phases has been found to be 3.05 g/cc for X-phase (ref. 18) and 3.08 g/cc for 15R polytype phase (ref. 18).

In general, the microstructures of both hot pressed and sintered materials consisted of  $\beta'$ -SiAlON as the predominant phase with some isolated porosity and metallic looking phase in a uniform  $\beta'$  matrix. In some cases isolated grains of X-phase and 15R polytype phases were also identified (ref. 10). Typical grain sizes of the hot pressed compositions were found to vary between 0.2 - 2  $\mu$ m (ref. 10) while the grain size range 0.15 - 5.0  $\mu$ m was observed in pressureless sintered compositions (ref. 31). The grain morphology in both sintered and hot pressed materials was characteristic of the presence of a liquid phase during densification. This liquid phase was retained in inter-crystalline spaces during cooling from the hot pressing (ref. 19) or sintering temperature (ref. 31) and formed a glassy phase at the grain boundaries.

#### PROPERTIES

Most of the mechanical properties reported in the literature are for  $\beta'$ -SiAlON in the system Si - Al - O - N, while other systems e.g. Si, Be/N, O; Si, Al Be/N, O etc., have been examined primarily with respect to solid solubility, phase relationships, and structure. Because of their similar structures, the physical and mechanical properties of  $\beta'$ -SiAlON and  $\beta'$ -Si<sub>3</sub>N<sub>4</sub> are also similar. In this review, the properties of various  $\beta'$ -SiAlON compositions in the system Si-Al-O-N are discussed.

##### Modulus of Rupture

Arrol (ref. 7) reported the room temperature modulus of rupture (3-point MOR) of a hot pressed  $\beta'$ -SiAlON to be as high as 825 MPa. He also reported the strength of sintered  $\beta'$ -SiAlON to be 330 MPa. The compositions or formulations of neither material were defined. Other workers have reported the MOR of hot pressed and sintered  $\beta'$ -SiAlONs where the formulations or compositions are defined to varying degrees. These are summarized in Table III. In Table III, average values at room temperature and at 1370 C are given for various  $\beta'$ -SiAlONs made from different starting materials. The highest room temperature strength of hot pressed  $\beta'$ -SiAlON bodies was found to be 648 MPa (ref. 17), while the highest strength obtained in pressureless sintered bodies was 483 MPa (ref. 31). At 1370 C, the highest MOR for sintered materials was 375 MPa (ref. 29). Only one value 240 (ref. 18) MPa is listed for a hot pressed  $\beta'$ -SiAlON at 1370 C.

Where data are available over a range of temperatures, the strength of sintered  $\beta'$ -SiAlONs is compared with the strength of silicon nitride currently produced in USA. This is shown in Fig. 8. As can be seen, the room temperature strength of sintered  $\beta'$ -SiAlON compares favorably with room temperature strength of sintered  $\text{Si}_3\text{N}_4$ . On the other hand, the room temperature strengths of sintered  $\beta'$ -SiAlON are considerably lower than the room temperature strength of hot pressed  $\text{Si}_3\text{N}_4$  (NC-132).

At high temperature (1370 C), the strength of sintered  $\beta'$ -SiAlON is equivalent to or higher than the strength of sintered  $\text{Si}_3\text{N}_4$  but lower than the strength of hot pressed  $\text{Si}_3\text{N}_4$  (NC-132).

The room temperature strength is controlled by residual porosity, surface flaws, foreign inclusions etc., in the body, while the high temperature strength is controlled by the grain boundary phases retained in the body during cooling from the sintering temperature. The grain boundary phase softens at high temperatures thus leading to slow crack growth and subsequent loss in strength. Fig. 9 shows an example of such typical slow crack growth failure (V-shaped area) in the fracture surfaces of a 1380 C MOR bar of  $\beta'$ -SiAlON sintered with 6 mol% ( $\text{Y}_2\text{O}_3 - \text{SiO}_2$ ) additive. Since the intended use of SiAlON has largely been for high temperature, high performance applications similar to those being attempted with  $\text{Si}_3\text{N}_4$  and SiC, improvement in strength at high temperature is desirable.

#### Creep

Limited creep data are available on  $\beta'$ -SiAlONs as compared with modulus of rupture data. Arrol (ref. 7) determined the creep behavior of several hot pressed SiAlONs, and compared the data with hot pressed  $\text{Si}_3\text{N}_4$  (HS-110) and (HS-130), hot pressed SiC and reaction bonded  $\text{Si}_3\text{N}_4$ . These are shown in Fig. 10. As can be seen, creep in the SiAlONs can vary depending on composition from a high value similar to that of HS-110 to a value as low as that of hot pressed SiC. Lumby et. al (ref. 33) compared the creep data of a pressureless sintered SiAlON with the data for various silicon based ceramics which are shown in Fig. 11. The sintered SiAlON has a creep rate lower than that of hot pressed  $\text{Si}_3\text{N}_4$  (HS-130), reaction bonded  $\text{Si}_3\text{N}_4$  or Refel SiC but slightly higher than that of hot pressed SiC. Lumby further observed a strong dependence of creep behavior on AlN concentration. Creep after 20 hours at 1227 C and 77 MN/m<sup>2</sup> decreased from 0.275% strain for a  $\beta'$ -SiAlON composition contained 7.75 wt% AlN down to 0.06% strain for a composition which contained 11.25% AlN (ref. 17).

According to Layden (ref. 9), three point flexural creep tests in argon of TLP sintered SiAlON gave a steady state creep rate of  $3.1 \times 10^{-4}$  hr<sup>-1</sup> at a stress level of 82 MN/m<sup>2</sup> at 1400 C. This value was below the compressional creep rate of hot pressed  $\text{Si}_3\text{N}_4$  under these conditions which has been reported (ref. 36) to be  $5.4 \times 10^{-3}$  hr<sup>-1</sup>. Layden also determined that the creep rate of the  $\text{Y}_2\text{O}_3$  containing  $\beta'$ -SiAlON bodies was about  $6 \times 10^{-5}$  hr<sup>-1</sup> at 1370 C and a stress level of 69 MN/m<sup>2</sup> which was comparable to that of commercial hot pressed  $\text{Si}_3\text{N}_4$  (HS-130) at the same stress and temperature. He observed that creep behavior was controlled by the properties of the grain boundary phases. For example,  $\beta'$ -SiAlON compositions containing  $\text{ZrO}_2$  additives exhibited slow crack growth during testing due to rapid flow of the grain boundary phases at stresses as low as 69 MN/m<sup>2</sup> at 1370 C. On the other hand,  $\beta'$ -SiAlON containing  $\text{Y}_2\text{O}_3$  exhibited higher refractoriness of the grain boundary phases. Therefore, no slow crack growth occurred during testing to 345 MN/m<sup>2</sup> at 1370 C and the specimens failed by fast fracture.

#### Fracture Toughness

Fracture toughness ( $K_{IC}$ ) values reported in the literature for various SiAlON compositions are listed in Table IV. Generally, the values are lower than those of hot pressed  $\text{Si}_3\text{N}_4$ . For example, Wills et. al (ref. 37) found the fracture toughness values varying between 1.32 and 2.65 MN/m<sup>-3/2</sup> as compared with 6 MN/m<sup>-3/2</sup> for (HS-130) hot pressed  $\text{Si}_3\text{N}_4$ . Wills also suggested that the presence of X - phase should be kept at very low levels and preferably be eliminated completely to improve the fracture toughness in SiAlONs. Similarly, Gauckler et. al (ref. 18) reported lower fracture toughness values (Table IV). However, Lumby et. al (ref. 33) observed a high fracture toughness value (6.0 MN/m<sup>-3/2</sup>) for a pressureless sintered SiAlON similar to (HS-130) hot pressed  $\text{Si}_3\text{N}_4$  as well as hot pressed SiAlON, measured by the same technique (ref. 33). He also determined the variation of fracture toughness with temperature for both hot pressed and sintered SiAlONs which is shown in Fig. 12. Lumby suggested that the increase in fracture toughness at higher temperatures was associated with the viscous deformation of the grain boundary phase. The variation in  $K_{IC}$  values shown in Table IV could probably be attributed to variation with SiAlON composition and fabrication techniques as well as variation with the fracture toughness measuring technique.

#### Oxidation

Oxidation resistance is one of the key properties that must be satisfied by a material in order to be candidate for high temperature applications. Jack (ref. 2) and Arrol (ref. 7) reported that the oxidation resistance of  $\beta'$ -SiAlONs is better than that of hot pressed  $\text{Si}_3\text{N}_4$  (HS-130). Layden (ref. 9) later confirmed this in his evaluation of oxidation behavior of TLP sintered SiAlON compositions. He observed that the oxidation rate of TLP  $\text{Si}_{1.4}\text{Al}_{1.6}\text{O}_{1.6}\text{N}_{2.4}$  was an order of magnitude less than that of (HS-130) hot pressed  $\text{Si}_3\text{N}_4$  at 1400 C (ref. 38). Layden (ref. 29) also made an ex-

tensive study on the oxidation behavior of  $\beta'$ -SiAlON compositions pressureless sintered with various additives such as  $\text{CeO}_2$ ,  $\text{Y}_2\text{O}_3$ ,  $\text{ZrO}_2$ ,  $\text{Y}_2\text{O}_3$ - $\text{ZrO}_2$ . These are shown in parabolic plots in Fig. 13 (ref. 29, 39).  $\text{CeO}_2$  doped material had the highest weight gain while TLP material (without any additive) had the lowest weight gain followed by  $\text{ZrO}_2$  doped SiAlON (Fig. 13). Both TLP and  $\text{ZrO}_2$  doped SiAlONS had much higher oxidation resistance than that of hot pressed  $\text{Si}_3\text{N}_4$  (HS-130). Similarly, Dutta (ref. 31) and Arias (ref. 30) reported a higher oxidation resistance in  $\beta'$ -SiAlONS doped with  $\text{Y}_2\text{O}_3$ - $\text{SiO}_2$  and  $\text{Y}_2\text{O}_3$  respectively, as compared with HS-130. Very recently, Arias (ref. 32) determined the oxidation resistance of SiAlON-C ( $\text{Si}_{2.55}\text{Al}_{0.60}\text{O}_{0.72}\text{N}_{3.52}$ ) to be even higher than that of TLP and  $\text{ZrO}_2$  doped SiAlONS. This is shown in Fig. 14. The oxidation behavior of several SiAlONS is compared with those of hot pressed silicon nitride (HS-130) produced commercially. All the sintered SiAlONS showed better oxidation resistance than hot pressed HS-130. This hot pressed  $\text{Si}_3\text{N}_4$  had the highest weight gain, while SiAlON - C (ref. 32) had the lowest weight gain followed by TLP SiAlON (ref. 9). The oxidation rate constant for SiAlON - C is  $2.5 \times 10^{-10} \text{ g}^2/\text{cm}^4 \text{ hr}^{-1}$  as compared with  $2.67 \times 10^{-8} \text{ g}^2/\text{cm}^4 \text{ hr}^{-1}$  for hot pressed  $\text{Si}_3\text{N}_4$  and  $1.96 \times 10^{-9} \text{ g}^2/\text{cm}^4 \text{ hr}^{-1}$  for TLP SiAlON, indicating that SiAlON compositions can be produced with excellent oxidation resistance as compared with this hot pressed  $\text{Si}_3\text{N}_4$ . However, these sintered SiAlONS such as SiAlON - C and TLP SiAlON have poor room temperature strength as compared with hot pressed  $\text{Si}_3\text{N}_4$ . For these materials to be accepted for turbine applications, further composition development is necessary to combine good oxidation behavior and good mechanical properties.

#### Thermal Expansion

Jack (ref. 2) reported the linear thermal coefficient of expansion of  $\beta'$ -SiAlON ( $\text{Si}_3\text{Al}_2\text{O}_4\text{N}_4$ ) to be  $2.7 \times 10^{-6} \text{ C}^{-1}$  which was less than that of  $\beta$ - $\text{Si}_3\text{N}_4$  ( $3.5 \times 10^{-6} \text{ C}^{-1}$ ). On the other hand, Gauckler et. al (ref. 18) reported an average value of  $3.4 \times 10^{-6} \text{ C}^{-1}$  which was in good agreement with the value for pure  $\beta$ - $\text{Si}_3\text{N}_4$ . Gauckler observed an almost linear decrease of the thermal expansion coefficient with increasing Al concentration for the  $\text{Si}_{6-x}\text{Al}_x\text{O}_x\text{N}_{8-x}$  SiAlON which is shown in Fig. 15.

Wills et. al (ref. 37) reported linear thermal expansion of three sintered SiAlON compositions. The expansion of the two compositions  $\text{Si}_{4.94}\text{Al}_{1.06}\text{O}_{1.06}\text{N}_{6.94}$  and  $\text{Si}_4\text{Al}_2\text{O}_2\text{N}_6$  was identical ( $3 \times 10^{-6} \text{ C}^{-1}$ ) but the third composition  $\beta' + X$  showed greater expansion ( $3.3 \times 10^{-6} \text{ C}^{-1}$ ) because of X - phase (ref. 37). However, collective data clearly indicated that the thermal expansion coefficients of  $\beta'$ -SiAlON compositions and of  $\beta$ - $\text{Si}_3\text{N}_4$  are quite similar.

#### Thermal Shock

Water quench thermal shock resistance ( $\Delta T_C^*$ ) of several SiAlONS determined by various investigators are listed in Table V along with data for other silicon based ceramics for comparison. The collective  $\Delta T_C$  values for  $\beta'$ -SiAlONS are comparable to those of various silicon carbide ceramics and reaction bonded silicon nitride. However, the values are considerably lower than that of hot pressed silicon nitride (Table V). Gauckler suggested that the poor thermal shock behavior of the  $\beta'$ -SiAlON despite its lower coefficient of thermal expansion was caused by the low thermal conductivity and poor fracture toughness of the material.

#### CONCLUDING REMARKS

The present review has shown that since the discovery of SiAlONS, a number of investigations have been made of their phase equilibria, structure, fabrication and properties. SiAlONS can be prepared by several chemical routes. Fully dense bodies can be produced by hot pressing, while a final density -98% of theoretical can be achieved by pressureless sintering. Both room temperature and high temperature strengths of sintered  $\beta'$ -SiAlONS are equivalent to or higher than the strengths of sintered silicon nitrides but lower than the strength of hot pressed silicon nitride (NC-132). On the other hand, many SiAlON compositions have higher oxidation resistance than those of hot pressed silicon nitrides, and therefore, have a better chance of longer survival in an oxidizing environment. However, the most significant lack in the current state of the art of SiAlON is that no SiAlON composition has yet been developed which exhibits good low temperature strength as well as good oxidation resistance. Indeed some of the SiAlONS that have exhibited the best oxidation resistance have also had low strength at high temperature. Only a few of the SiAlONS identified to date hold promise for high temperature use in gas turbines. Because of their low strength at lower temperature, it is not likely that sintered SiAlONS nor sintered silicon nitride will be used for integrally bladed turbine wheels. Such wheels are highly stressed in the lower temperature region of the hub. To date hot pressed  $\text{Si}_3\text{N}_4$  has been the favored material. However, SiAlON materials have the advantage of pressureless sintering to high density and thereby have the potential for providing low cost net shape components to intricate geometry without expensive machining.

\* $\Delta T_C$  - critical quenching-temperature difference required to initiate thermal stress fracture (see ref. 41 for more detailed explanation).

At present, a more likely use for sintered SiAlONs in the turbine is for stator vanes which run hotter, and at lower stresses than turbine blades or disks. For those SiAlONs that have potential for use in gas turbines, much work remains to be done to characterize them in the depth required for such an application.

It is to be hoped that improvement in mechanical properties can be achieved in combination with good oxidation resistance by choosing proper chemical formulations. Work to date indicates that such a combination can be best achieved at low Al<sub>2</sub>O<sub>3</sub> concentrations. However, to select an optimum composition, a clear understanding of the phase equilibria of the particular system is essential.

#### REFERENCES

1. Y. Oyama and O. Kamigaito, "Solid Solubility of Some Oxides in Si<sub>3</sub>N<sub>4</sub>," Jap. J. Appl. Phys., 10, 1971, p. 1637.
2. K. H. Jack and W. I. Wilson, "Ceramics Based on the Si-Al-O-N Related Systems," Nature Phys. Sci., 238, 1972, pp. 28-29.
3. Y. Oyama, "Solid Solution in the Ternary System, Si<sub>3</sub>N<sub>4</sub>-AlN-Al<sub>2</sub>O<sub>3</sub>," Jap. J. Appl. Phys., 11, 1972, pp. 750-751.
4. K. H. Jack, "SiAlONs and Related Nitrogen Ceramics," J. Mat. Sci., 11, 1976, pp. 1135-1158.
5. K. H. Jack, "Nitrogen Ceramics," Trans. J. Brit. Ceram. Soc., 72, 1973, pp. 376-384.
6. Y. Oyama, "Solid Solution in the System Si<sub>3</sub>N<sub>4</sub> - Ga<sub>2</sub>O<sub>3</sub>-Al<sub>2</sub>O<sub>3</sub>," Jap. J. Appl. Phys., 12, 1973, pp. 500-508.
7. W. J. Arrol, "The SiAlONs - Properties and Fabrication," Ceramics for High Performance Applications, Edited by J. J. Burke, A. E. Gorum, and R. N. Katz, Chestnut Hill, Mass., Brook Hill Publishing Co., 1974, pp. 729-738.
8. L. J. Gauckler, H. L. Lukas, and G. Petzow, "Contribution to the Phase Diagram Si<sub>3</sub>N<sub>4</sub>-AlN-Al<sub>2</sub>O<sub>3</sub>-SiO<sub>2</sub>," J. Amer. Cer. Soc., 58, 1975, pp. 346-347.
9. G. K. Layden, "Pressureless Sintering of SiAlON Gas Turbine Components," East Hartford, Conn., United Technologies Research Center, 1977. Warminster, Pa., Naval Air Development Center, NADC-75207-30, 1979.
10. P. Drew and M. H. Lewis, "The Microstructures of Silicon Nitride/Alumina Ceramics," J. Mat. Sci., 9, 1974, pp. 1833-1838.
11. E. Gugel, I. Petzenhauser, and A. Fickel, "X-Ray Investigation of the System Si<sub>3</sub>N<sub>4</sub>-Al<sub>2</sub>O<sub>3</sub>," Powder Metall. Int., 7, 1975, pp. 66-67.
12. I. C. Huseby, H. L. Lukas, and G. Petzow, "Phase Equilibria in the System Si<sub>3</sub>N<sub>4</sub>-SiO<sub>2</sub>-BeO-Be<sub>3</sub>N<sub>2</sub>," J. Amer. Cer. Soc., 58, 1975, pp. 377-380. (1975)
13. L. J. Gauckler and G. Petzow, "Representation of Multicomponent Silicon Nitride Based Systems," Nitrogen Ceramics, Edited by F. L. Riley, NATO Advanced Study Institute, Noordhoff, Leyden, The Netherlands, 1976, pp. 41-62.
14. Y. Oyama and O. Kamigaito, "Hot Pressing of Si<sub>3</sub>N<sub>4</sub>-Al<sub>2</sub>O<sub>3</sub>," Yogyo-Kyokai-Shi, 80, 1972, pp. 327-336.
15. F. F. Lange, "Fabrication and Properties of Silicon Compounds, Task 1, Fabrication, Microstructure and Selected Properties of SiAlON Compositions," Pittsburgh, Pa., Westinghouse Research Labs., 1974, pp. 1-23.
16. W. B. Crandall, A. Z. Hed, L. E. Shipley, "Preparation and Evaluation of SiAlON," Wright-Patterson AFB, Ohio, Aerospace Research Labs., ARL-TR-74-99, 1973.
17. R. J. Lumby, B. North and A. J. Taylor, "Chemistry and Creep of SiAlONs," Special Ceramics, Vol 6, Edited by P. Popper, Manchester, England, British Ceramic Research Assoc., 1975, pp. 283-298.
18. L. J. Gauckler, S. Prietzel, G. Bodemer, and G. Petzow, "Some Properties of  $\beta$ -Si<sub>6-x</sub>Al<sub>x</sub>O<sub>x</sub>N<sub>8-x</sub>," Nitrogen Ceramics, Edited by F. L. Riley, NATO Advanced Study Institute, Noordhoff, Leyden, The Netherlands, 1977, pp. 529-538.
19. M. H. Lewis, B. D. Powell, P. Drew, R. J. Lumby, B. North, and A. J. Taylor, "The Formation of Single-Phase Si-Al-O-N Ceramics," J. Mat. Sci., 12, 1977, pp. 61-74.
20. H. C. Yeh and W. J. Waters, "Effects of Pressure and Temperature on Hot Pressing a SiAlON," NASA TM-78945, 1977.



21. P. L. Land and S. Holmquist, "Evaluation of  $\beta$ -SiAlON for Radome Application," Wright-Patterson AFB, Ohio, Air Force Materials Lab., AFML-TR-78-79, 1978.
22. W. M. Phillips and Y. S. Kuo, " SiAlONs as High Temperature Insulators," Pasadena, Calif., Jet Propulsion Lab., MPL-Publ-78-103, 1978.
23. H. C. Yeh, W. A. Sanders and J. L. Fiyalko-Liettnr, "Pressure Sintering of  $\text{Si}_3\text{N}_4\text{-Al}_2\text{O}_3$  (SiAlON)," Amer. Ceram. Soc. Bul., 56, 1977, pp. 189-193.
24. P. E. D. Morgan, "Amorphous Silicon Nitride and a Classification of SiAlON," Amer. Ceram. Soc. Bull. 53, 1974, Abstract 4-S2-74, p. 392.
25. L. J. Gauckler, S. Boskovic, I. K. Naik, and T. Y. Tien, "Liquid Phase Sintering of  $\beta$ - $\text{Si}_3\text{N}_4$  Solid Solutions Containing Alumina," Ceramics for High Performance Applications-II, Edited by J. J. Burke, E. N. Lenoe, R. N. Katz, Chestnut Hill, Mass., Brook Hill Publ. Co., 1978, pp. 559-571.
26. A. Arias, "Effect of Oxygen to Nitrogen Ratio on the Sinterability of SiAlONs," NASA TP-1382, 1979.
27. A. Gatti and M. J. Noone, "Methods of Fabricating Materials," Wright-Patterson AFB, Ohio, Air Force Materials Lab., AFML-TR-77-135, 1977.
28. R. R. Wills, R. W. Stewart and J. M. Wimmer, "Fabrication of Reaction-Sintered SiAlON," J. Am. Ceram. Soc., 60, 1977, pp. 64-67.
29. G. K. Layden, "Development of SiAlON Materials," NASA CR-135290, 1977, East Hartford, CT, United Technologies Research Center, R77-912184-21, 1977. NASA CR-135290, 1977.
30. A. Arias, "Pressureless Sintered SiAlONs with Low Amounts of Sintering Aid," NASA TP-1246, 1978.
31. S. Dutta, "Pressureless Sintered  $\beta'$ - $\text{Si}_3\text{N}_4$  Solid Solution: Fabrication, Microstructure and Strength, NASA TM-78950, 1977.
32. A. Arias, "Modulus of Rupture and Oxidation Resistance of a  $\text{Si}_{2.55}\text{Al}_{0.60}\text{O}_{0.72}\text{N}_{3.52}$  SiAlON," NASA TP-1490 1979.
33. R. J. Lumby, B. North and A. J. Taylor, "Properties of Sintered SiAlONs and Some Applications in Metal Handling and Cutting," Ceramics for High Performance Applications-II, Edited by J. J. Burke, E. N. Lenoe, and R. N. Katz, Chestnut Hill, Mass., Book Hill Publishing Company, 1978, pp. 893-906.
34. D. C. Larsen and G. C. Walther, "Property Screening and Evaluation of Ceramic Turbine Engine Materials," Chicago, Ill., IIT Research Inst., IITRI-D6114-ITR-36, (Interim Tech. Report No. 6), July 1978.
35. S. Dutta, "Microstructure and Property Characterization of Sintered  $\text{Si}_3\text{N}_4$ , SiC and SiAlON," Ceram. Soc. Bull. 58, 1979, Abstract 102-B-79, p. 348.
36. M. S. Seltzer, "High Temperature Creep of Ceramics", Wright-Patterson AFB, Ohio, Air Force Materials Lab., AFML-TR-76-97, 1976. (AD-A031766)
37. R. R. Wills, R. W. Stewart, and J. M. Wimmer, "Effect of Composition and X-phase on the Intrinsic Properties of Reaction-Sintered SiAlON," Am. Ceram. Soc. Bull. 56, 1977, pp. 194-198.
38. W. C. Tripp and H. C. Graham, "Oxidation of  $\text{Si}_3\text{N}_4$  in the Range 1300 to 1500 C," J. Am. Ceram. Soc., 59, 1976, pp. 399-403.
39. R. L. Ashbrook, "Improved Performance of Silicon Nitride-Based High Temperature Ceramics," NASA TM 73719, 1977.
40. C. C. Seaton, "Thermal and Acoustic Fatigue of Ceramics and Their Evaluation," Watertown, Mass., Army Materials and Mechanics Research Center, AMMRC-MS-74-7, 1974. (AD-785547)
41. D. P. H. Hasselman, "Unified Theory of Thermal Shock Fracture Initiation and Crack Propagation in Brittle Ceramics," J. Am. Ceram. Soc. 52, 1969, pp. 600-604.

TABLE I. - FABRICATION OF SIALONS BY HOT PRESSING

Starting materials	Additives	Temperature, C	Time, min	Pressure, MN/m <sup>2</sup>	Nature of investigation	Reference	
Si <sub>3</sub> N <sub>4</sub> , Al <sub>2</sub> O <sub>3</sub> , Li <sub>2</sub> CO <sub>3</sub>	(a)	1750	20	29	Solid solubility	1	
Si <sub>3</sub> N <sub>4</sub> , Al <sub>2</sub> O <sub>3</sub>	↓	1700	60	(a)	Formation, structure and thermal expansion	2	
Si <sub>3</sub> N <sub>4</sub> , AlN, Al <sub>2</sub> O <sub>3</sub>		1730	30	25	Solid solubility	3	
Si <sub>3</sub> N <sub>4</sub> , Ga <sub>2</sub> O <sub>3</sub> , Al <sub>2</sub> O <sub>3</sub>		1730-1800	20-180	25	Solid solubility and thermal expansion	5	
Si <sub>3</sub> N <sub>4</sub> , Al <sub>2</sub> O <sub>3</sub> , AlN, SiO <sub>2</sub>		1760	60-300	30	Phase equilibria and compatibility relation	7	
Si <sub>3</sub> N <sub>4</sub> , AlN, Al <sub>2</sub> O <sub>3</sub> , SiO <sub>2</sub> , Si <sub>2</sub> N <sub>2</sub> O		1500-2000	(a)	(a)	Phase equilibria, compatibility and structure	8	
Si <sub>3</sub> N <sub>4</sub> , Al <sub>2</sub> O <sub>3</sub>		1700	60	15	Microstructure and phase analysis	10	
Si <sub>3</sub> N <sub>4</sub> , Al <sub>2</sub> O <sub>3</sub>		1700	30	(a)	Phase analysis	11	
Si <sub>3</sub> N <sub>4</sub> , Be <sub>3</sub> N <sub>2</sub> , BeO, SiO <sub>2</sub>		1765-1880	60-120	28	Phase equilibria	12	
Si <sub>3</sub> N <sub>4</sub> , Al <sub>2</sub> O <sub>3</sub>		1650-1850	6-60	25	Sintering, grain growth and phase equilibria	14	
Si <sub>3</sub> N <sub>4</sub> , Al <sub>2</sub> O <sub>3</sub>		MgO	1750-1850	30-240	28	Fabrication, modulus of rupture and thermal properties	15
Si <sub>3</sub> N <sub>4</sub> , Al <sub>2</sub> O <sub>3</sub>		Si, Al, MgO, AlN, SiO <sub>2</sub> , Kaolin	1500-2000	1-1440	28	Processing and properties	16
Si <sub>3</sub> N <sub>4</sub> , AlN, SiO <sub>2</sub>		MgO	1750	60	20	Fabrication, chemistry and creep	17
Si <sub>3</sub> N <sub>4</sub> , Al <sub>2</sub> O <sub>3</sub> , AlN, SiO <sub>2</sub>	MgO	1760	(a)	(a)	Physical, mechanical and thermal properties	18	
Si <sub>3</sub> N <sub>4</sub> , AlN, SiO <sub>2</sub>	MgO	1800	60	15	Formation, microstructure characterization	19	
Si <sub>3</sub> N <sub>4</sub> , Al <sub>2</sub> O <sub>3</sub>	(a)	1500-1700	120	5.5-27.5	Effects of pressure and temperature on sintering	20	
Si <sub>3</sub> N <sub>4</sub> , AlN, Al <sub>2</sub> O <sub>3</sub>	(a)	1600-1800	5-60	3.5-22	Modulus of rupture, dielectric properties and rain erosion	21	
Si <sub>3</sub> N <sub>4</sub> , AlN, Al <sub>2</sub> O <sub>3</sub>	MgO	1700-1870	30-120	13.8-34.5	Electrical resistivity and compatibility with W and Mo	22	
Si <sub>3</sub> N <sub>4</sub> , Al <sub>2</sub> O <sub>3</sub>	(a)	1200-1700	120	27.6	Hot pressing and microstructure characterization	23	

<sup>a</sup>Not reported.

TABLE II. - FABRICATION OF SIAlONS BY PRESSURELESS SINTERING

Starting materials	Additives	Temperature, C	Time, min	Nature of investigation	Reference
$Si_3N_4, Al_2O_3$	(a)	1700	60	Fabrication (slip casting) and sintering	2
$Si_3N_4, Al_2O_3$		1600-1850	15-720	Fabrication, modulus of rupture, creep, impact oxidation	9
$Si_3N_4, Al_2O_3$		1400-1800	60	Microstructure analysis	10
$Si_3N_4, Al_2O_3$		(a)	(a)	Phase analysis	11
$Si_3N_4, AlN, Al_2O_3$		1400-2000	0-180	Liquid phase sintering	25
$Si_3N_4, AlN, SiO_2$		1670-1830	240	Effect of oxygen to nitrogen ratio on densification	26
$Si_3N_4, Al_2O_3, AlN$		1775-1800	60	Fabrication and modulus of rupture	27
$Si_3N_4, AlN, Al_2O_3$		1740	60	Fabrication and modulus of rupture	28
$\beta'$ -SiAlON	$CeO_2, Y_2O_3, ZrO_2, AlPO_4, GaPO_4, ZrC, La_2O_3, Er_2O_3, Nd_2O_3 (Sm, Gd)O_3$	1700-1800	60-180	Fabrication, modulus of rupture, creep and oxidation	29
$Si_3N_4, SiO_2, AlN$	$Y_2O_3$	1760	240	Fabrication, modulus of rupture and oxidation	30
$Si_3N_4, AlN, Al_2O_3$	$Y_2O_3-SiO_2$	1450-1750	60-120	Fabrication, modulus of rupture and oxidation	31
$Si_3N_4, AlN, Al_2O_3$	$Y_2O_3, MgO-Y_2O_3, MgAl_2O_4$	1750	240	Fabrication, modulus of rupture and oxidation	Current work by the author

not reported.

TABLE III. - MODULUS OF RUPTURE OF HOT-PRESSED AND SINTERED SIALONS

Starting materials <sup>b</sup>	Basic formula	Fabrication method	Average 4-point modulus of rupture, MPa		Reference
			25° C	1370° C	
Si <sub>3</sub> N <sub>4</sub> , Al <sub>2</sub> O <sub>3</sub>	Si <sub>3</sub> Al <sub>2.67</sub> O <sub>4</sub> N <sub>4</sub>	Hot-pressed	310	a	4
Si <sub>3</sub> N <sub>4</sub> , Al <sub>2</sub> O <sub>3</sub>	<sup>a</sup>	→	420	a	15
Si <sub>3</sub> N <sub>4</sub> , AlN, Al <sub>2</sub> O <sub>3</sub> , SiO <sub>2</sub> (MgO)	Si <sub>2.67</sub> Al <sub>1.30</sub> O <sub>4.43</sub> N <sub>3.57</sub>	→	648	a	17
Si <sub>3</sub> N <sub>4</sub> , AlN, Al <sub>2</sub> O <sub>3</sub>	Si <sub>2.25</sub> Al <sub>0.75</sub> O <sub>3.25</sub> N <sub>3.25</sub>	→	510	c240	18
Si <sub>3</sub> N <sub>4</sub> , Al <sub>2</sub> O <sub>3</sub>	<sup>a</sup>	Sintered	250	a	15
Si <sub>3</sub> N <sub>4</sub> , AlN, SiO <sub>2</sub>	Si <sub>1.4</sub> Al <sub>1.6</sub> O <sub>1.6</sub> N <sub>2.4</sub>	→	208	180	9
Si <sub>3</sub> N <sub>4</sub> , AlN, Al <sub>2</sub> O <sub>3</sub>	Si <sub>4</sub> Al <sub>2</sub> O <sub>2</sub> N <sub>6</sub>	→	352	135	28
Basic β'(Y <sub>2</sub> O <sub>3</sub> )	Si <sub>2.45</sub> Al <sub>0.55</sub> O <sub>3.45</sub> N <sub>3.45</sub>	→	450	335	29
β'(Y <sub>2</sub> O <sub>3</sub> )	Si <sub>2.7</sub> Al <sub>0.3</sub> O <sub>3.7</sub> N <sub>3.7</sub>	→	460	375	→
β'(CeO <sub>2</sub> )	Si <sub>2.45</sub> Al <sub>0.55</sub> O <sub>3.45</sub> N <sub>3.45</sub>	→	400	a	→
β'(ZrO <sub>2</sub> )	Si <sub>2.45</sub> Al <sub>0.55</sub> O <sub>3.45</sub> N <sub>3.45</sub>	→	430	235	→
Si <sub>3</sub> N <sub>4</sub> , AlN, SiO <sub>2</sub> (Y <sub>2</sub> O <sub>3</sub> )	Si <sub>2.6</sub> Al <sub>0.39</sub> O <sub>4.36</sub> N <sub>3.6</sub>	→	460	175	30
Si <sub>3</sub> N <sub>4</sub> , AlN, Al <sub>2</sub> O <sub>3</sub> (Y <sub>2</sub> O <sub>3</sub> -SiO <sub>2</sub> )	Si <sub>2.4</sub> Al <sub>0.8</sub> O <sub>3.6</sub> N <sub>3.6</sub>	→	483	228	31
Si <sub>3</sub> N <sub>4</sub> , AlN, SiO <sub>2</sub>	Si <sub>2.55</sub> Al <sub>0.6</sub> O <sub>3.52</sub> N <sub>3.52</sub>	→	404	260	32
Si <sub>3</sub> N <sub>4</sub> , AlN, SiO <sub>2</sub> (MgO)	<sup>a</sup>	→	410	310	33
Si <sub>3</sub> N <sub>4</sub> , AlN, Al <sub>2</sub> O <sub>3</sub> (Y <sub>2</sub> O <sub>3</sub> )	Si <sub>1.8</sub> Al <sub>1.6</sub> O <sub>1.5</sub> N <sub>3.0</sub>	→	404	65	Current work by the author
	Si <sub>2.07</sub> Al <sub>1.24</sub> O <sub>1.2</sub> N <sub>3.2</sub>	→	305	69	→
	Si <sub>2.4</sub> Al <sub>0.8</sub> O <sub>3.4</sub> N <sub>3.4</sub>	→	295	95	→
	Si <sub>2.2</sub> Al <sub>1.08</sub> O <sub>1.08</sub> N <sub>3.28</sub>	→	395	135	→

<sup>a</sup>Not reported.<sup>b</sup>The additive or sintering aid is enclosed in parentheses.<sup>c</sup>3-point MOR.

TABLE IV. - FRACTURE TOUGHNESS ( $K_{Ic}$ ) OF SIALON MATERIALS

Starting materials	Basic formula	Fabrication method	Fracture toughness (25° C) $MN/m^{-3/2}$	Reference
$Si_3N_4, Al_2O_3$	a	Hot-pressed	1-2	15
$Si_3N_4, AlN, SiO_2$	$Si_{2.25}Al_{0.75}O_{0.75}N_{3.25}$	Hot-pressed	4	18
$Si_3N_4, MgO$	$Si_3N_4$ (HS-130)	Hot-pressed	6.0	33
$Si_3N_4, AlN, SiO_2$ (MgO)	a	Sintered	6.0	33
$Si_3N_4, AlN, Al_2O_3$	$Si_4Al_2O_2N_6$	Sintered	2.2-2.7	37
a, X	a	Sintered	1.32	37

<sup>a</sup>Not reported.

TABLE V. - WATER QUENCH THERMAL SHOCK RESISTANCES ( $\Delta T_c$ ) OF SIALON,  $Si_3N_4$  and SiC CERAMICS

Material	Basic formula	$\Delta T_c$	Reference
Hot-pressed SIALON	$Si_{2.25}Al_{0.75}O_{0.75}N_{3.25}$	320	18
Sintered SIALON	$Si_{2.4}Al_{0.8}O_{0.6}N_{3.6}$	460-480	31
Sintered SIALON	a	510	33
Reaction sintered SiC	SiC	305	40
Hot pressed SiC	SiC	415	40
Reaction sintered $Si_3N_4$	$Si_3N_4$	510	40
Hot pressed $Si_3N_4$	$Si_3N_4$	750	18

<sup>a</sup>Not reported.

E-012

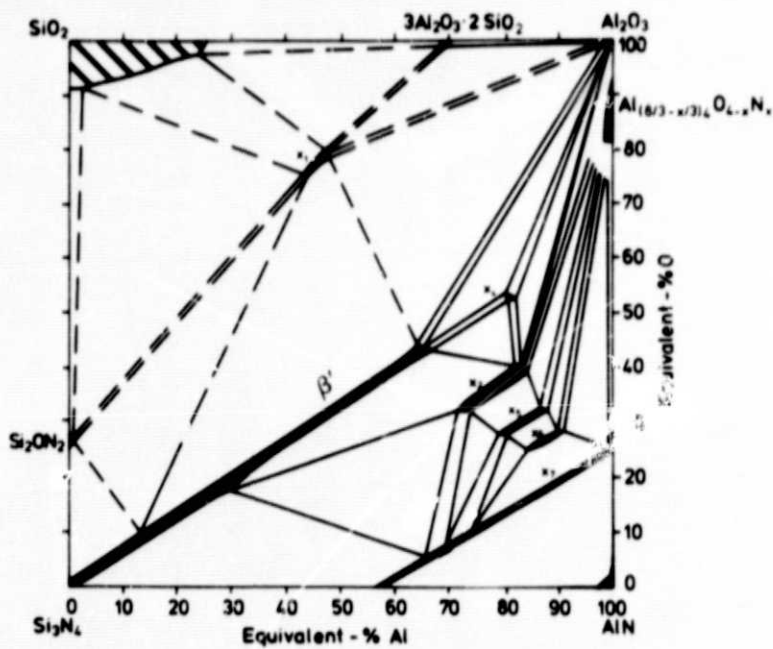
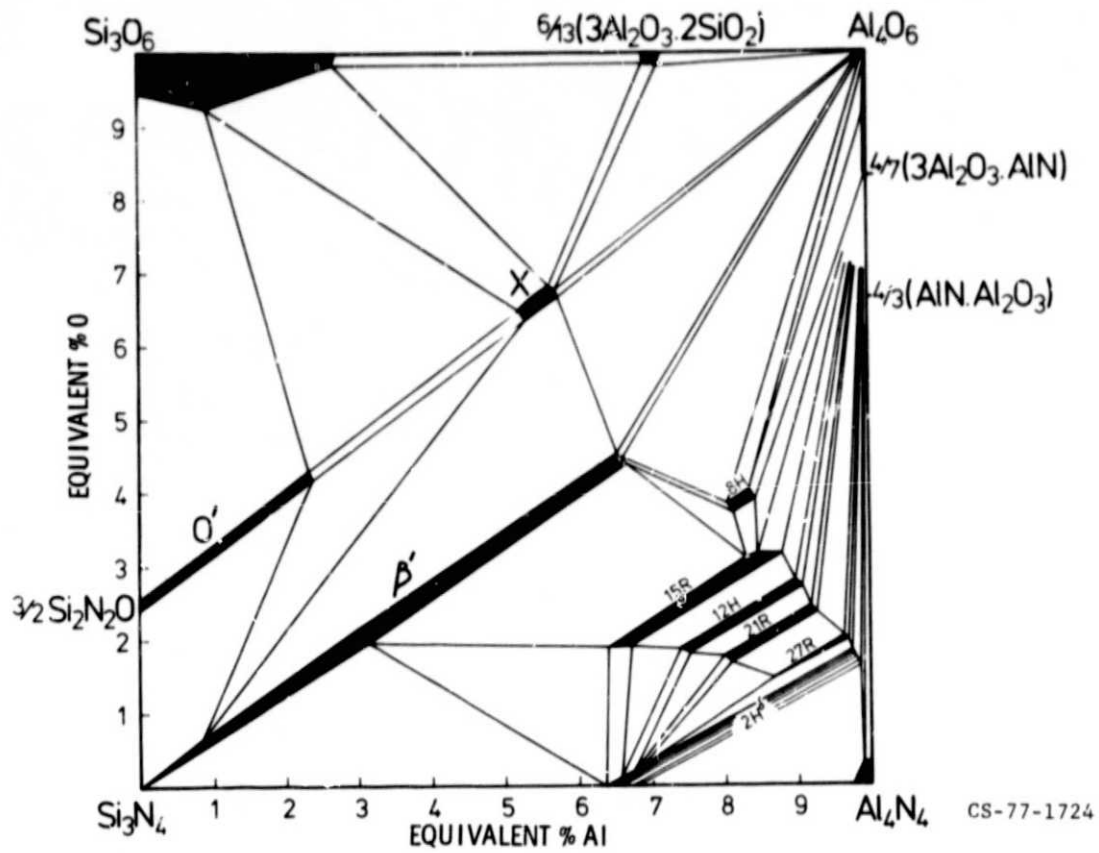


Figure 1. - Isothermal section  $\text{Si}_3\text{N}_4$  -  $\text{AlN}$  -  $\text{Al}_2\text{O}_3$  -  $\text{SiO}_2$  of the system Si-Al-O-N at 1760°C (ref. 8).



CS-77-1724

Figure 2. - The  $\text{Si}_3\text{N}_4$ -AlN- $\text{Al}_2\text{O}_3$ - $\text{SiO}_2$  system (ref. 4).

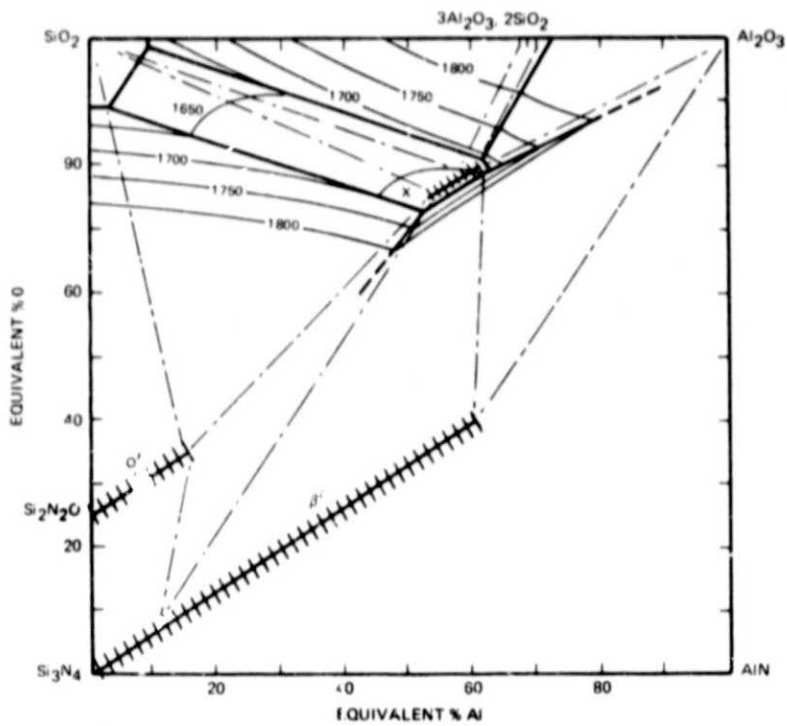


Figure 3. - The  $\text{Si}_3\text{N}_4$ - $\text{AlN}$ - $\text{Al}_2\text{O}_3$ - $\text{SiO}_2$  system showing liquidus isotherms ( $1650^\circ$  -  $1800^\circ$  C) between the  $\text{SiO}_2$  corner and X-phase (ref. 9).

F-12

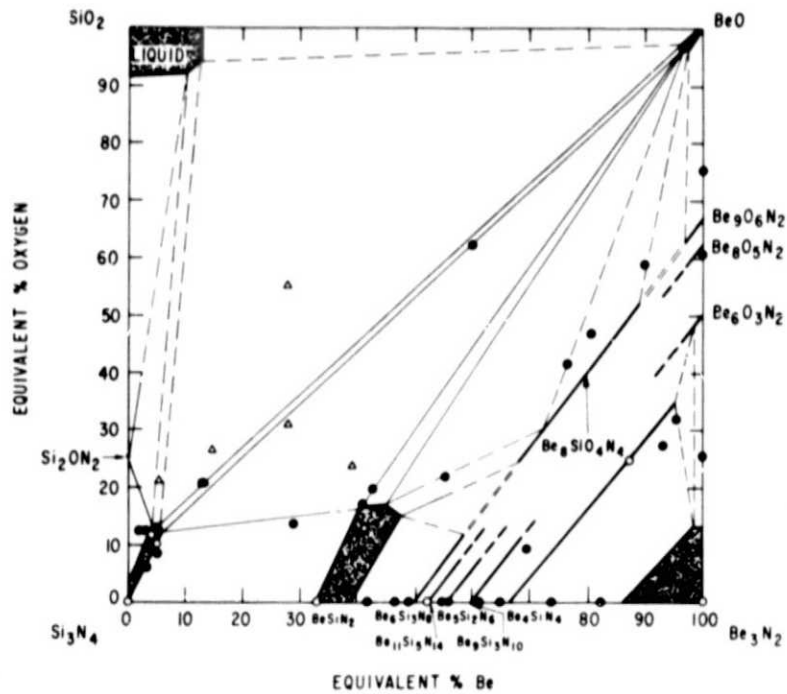


Figure 4. - Isothermal section of the system  $\text{Si}_3\text{N}_4$ - $\text{SiO}_2$ - $\text{BeO}$ - $\text{Be}_3\text{N}_2$  at  $1780^\circ$  C (ref. 12).



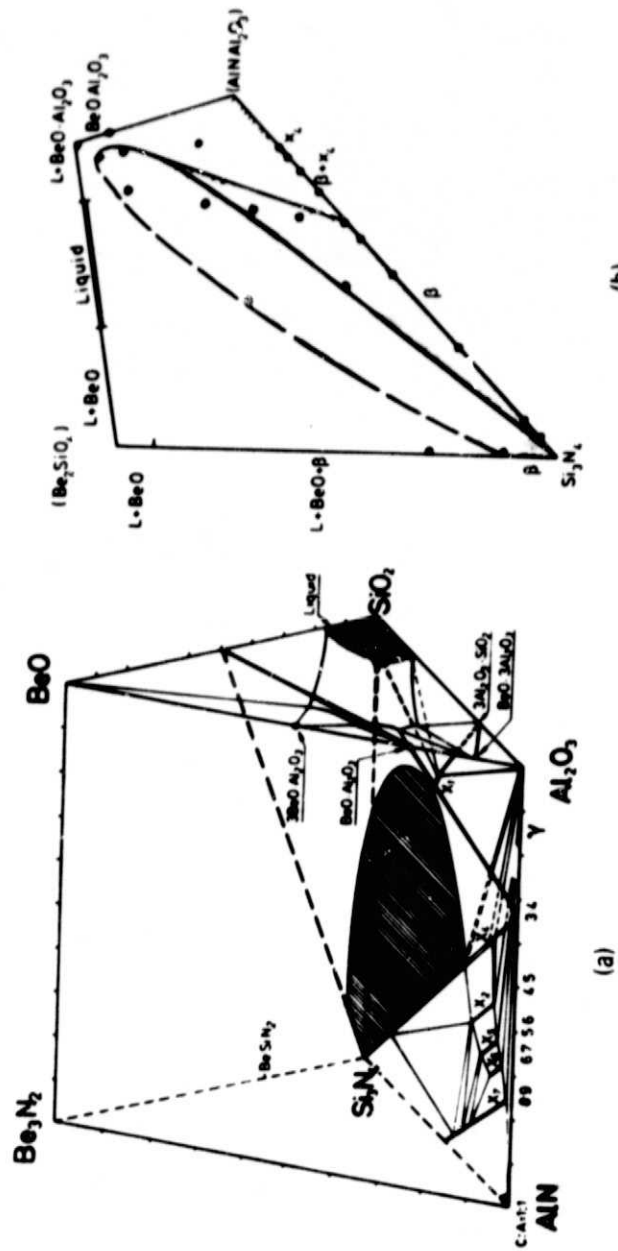


Figure 5. - Phase diagram of the quaternary system  $\text{Si}_3\text{N}_4$  -  $\text{AlN}$  -  $\text{Al}_2\text{O}_3$  -  $\text{Be}_3\text{N}_2$  -  $\text{BeO}$  at  $1760^\circ\text{C}$  (ref. 13).

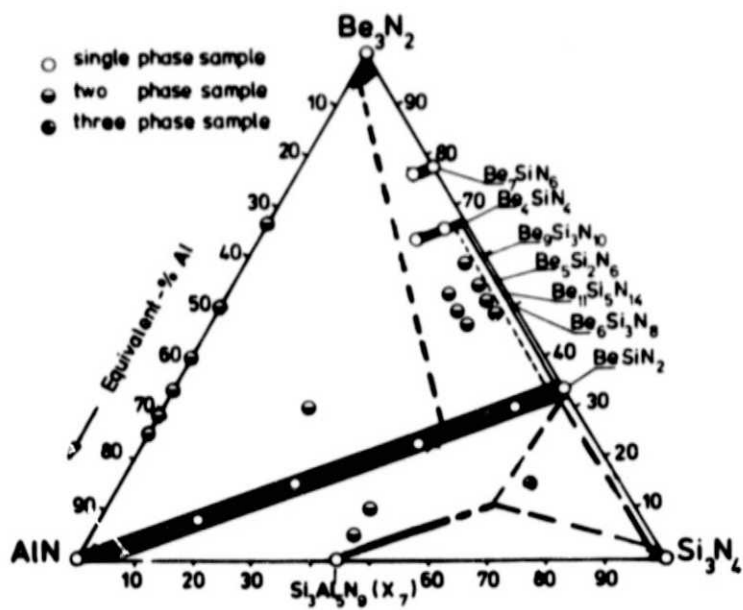


Figure 6. - The systems Si-Al-Be-N at 1780<sup>o</sup> C (ref. 13).

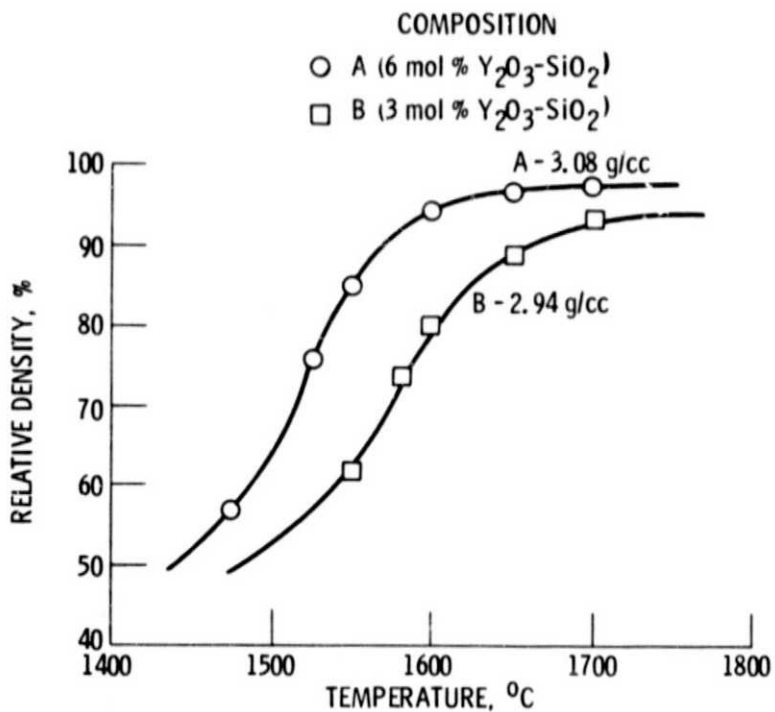


Figure 7. - Density of sintered  $\beta'$  - SiAlON for 1 hour at different temperatures (ref. 31).

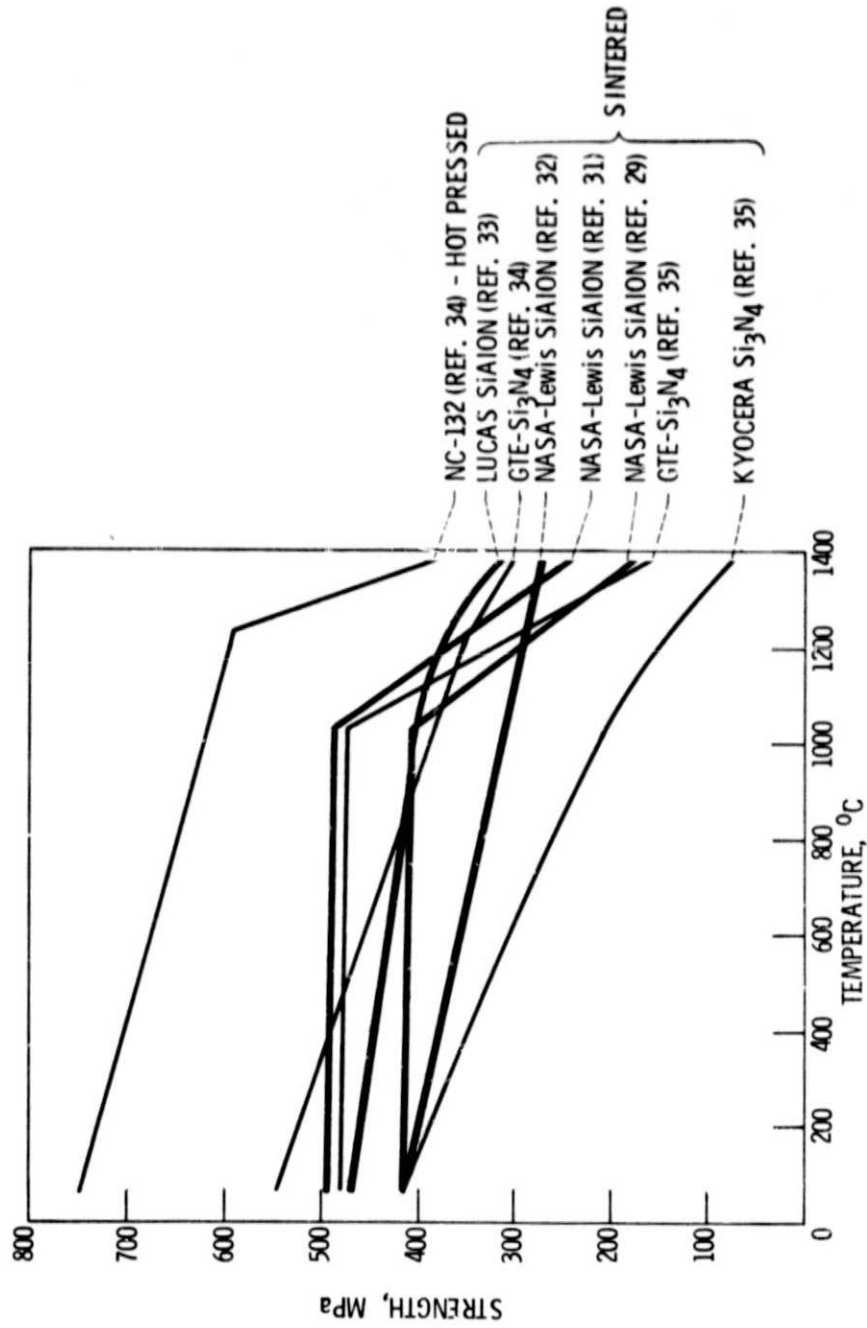


Figure 8. - Comparison of strength behavior of  $\beta'$  SIAION and  $Si_3N_4$  materials.

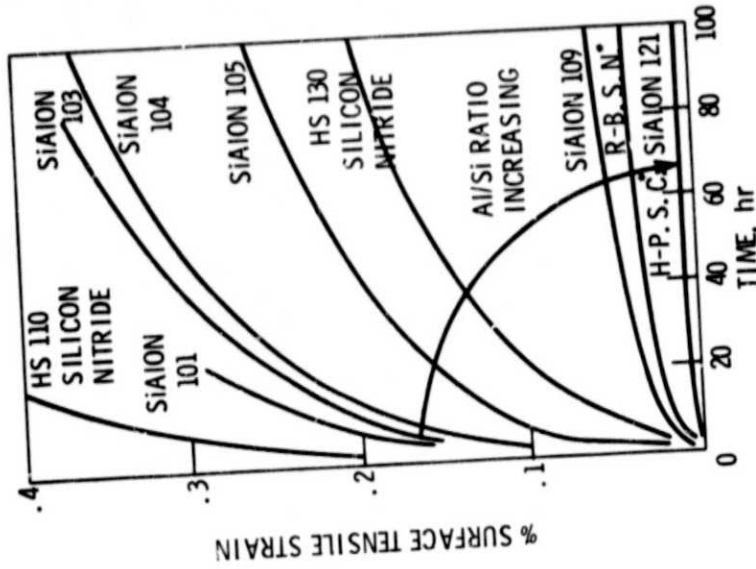
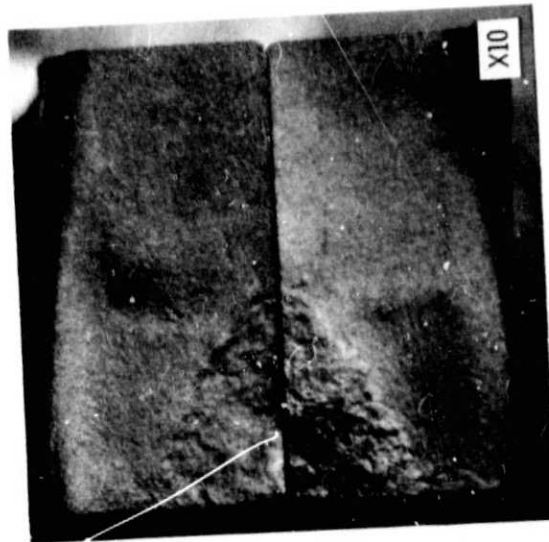


Figure 10. - Creep of various ceramic materials. 1227° C, 77 MNV/m<sup>2</sup>. (After Arrol<sup>7</sup>).

\* Composition not defined.



A - 6 mol% Y<sub>2</sub>O<sub>3</sub>-SiO<sub>2</sub>

Figure 9. - Fracture surface (1380° C) of sintered β'-SiAlON (Si<sub>2</sub>Al<sub>0.8</sub>O<sub>0.6</sub>N<sub>3.6</sub>) bend bar. V-shaped area indicates slow crack growth (ref. 31).

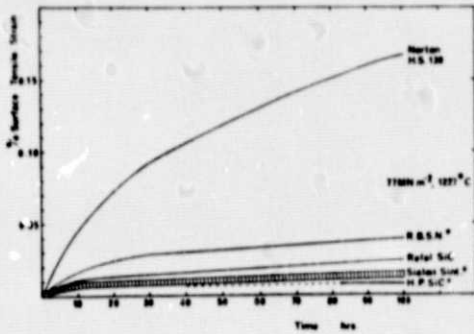


Figure 11. - Comparison of creep (4-pt. bend) behavior of  $\text{Si}_3\text{N}_4$ , SiC, and SiAlON (ref. 33).

\* Composition not defined.

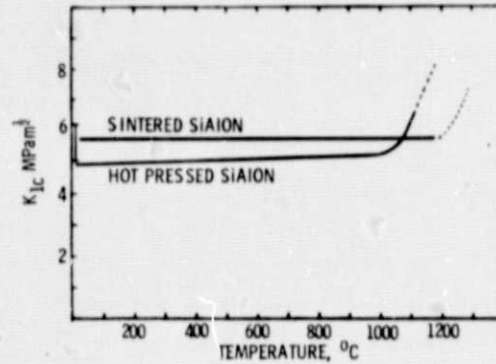


Figure 12. - Variation of fracture toughness with temperature for hot-pressed and sintered SiAlONs (ref. 33).

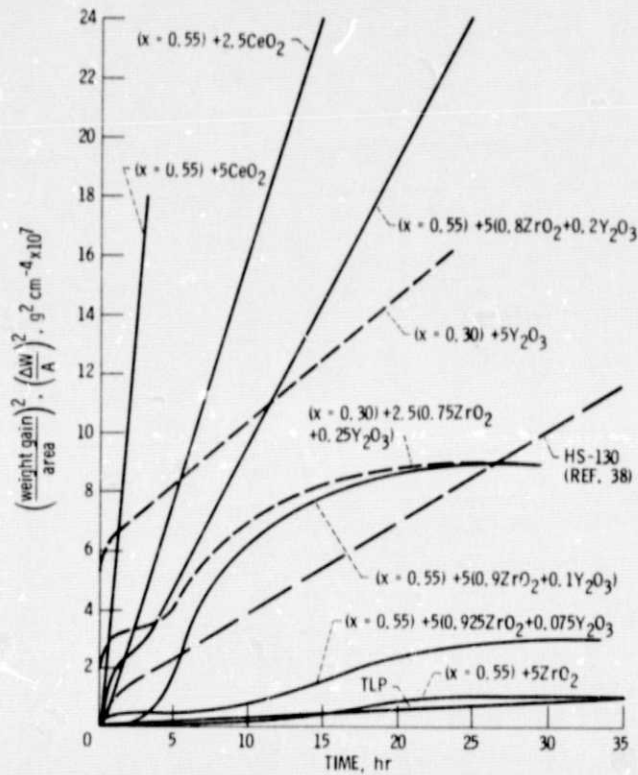


Figure 13. - Weight gain in air at  $1400^\circ\text{C}$  ( $2550^\circ\text{F}$ ) of various SiAlON compositions ( $\text{Si}_{3-x}\text{Al}_x\text{O}_4\text{N}_{4-x}$ ) after Layden (ref. 29) and Ashbrook (ref. 39).

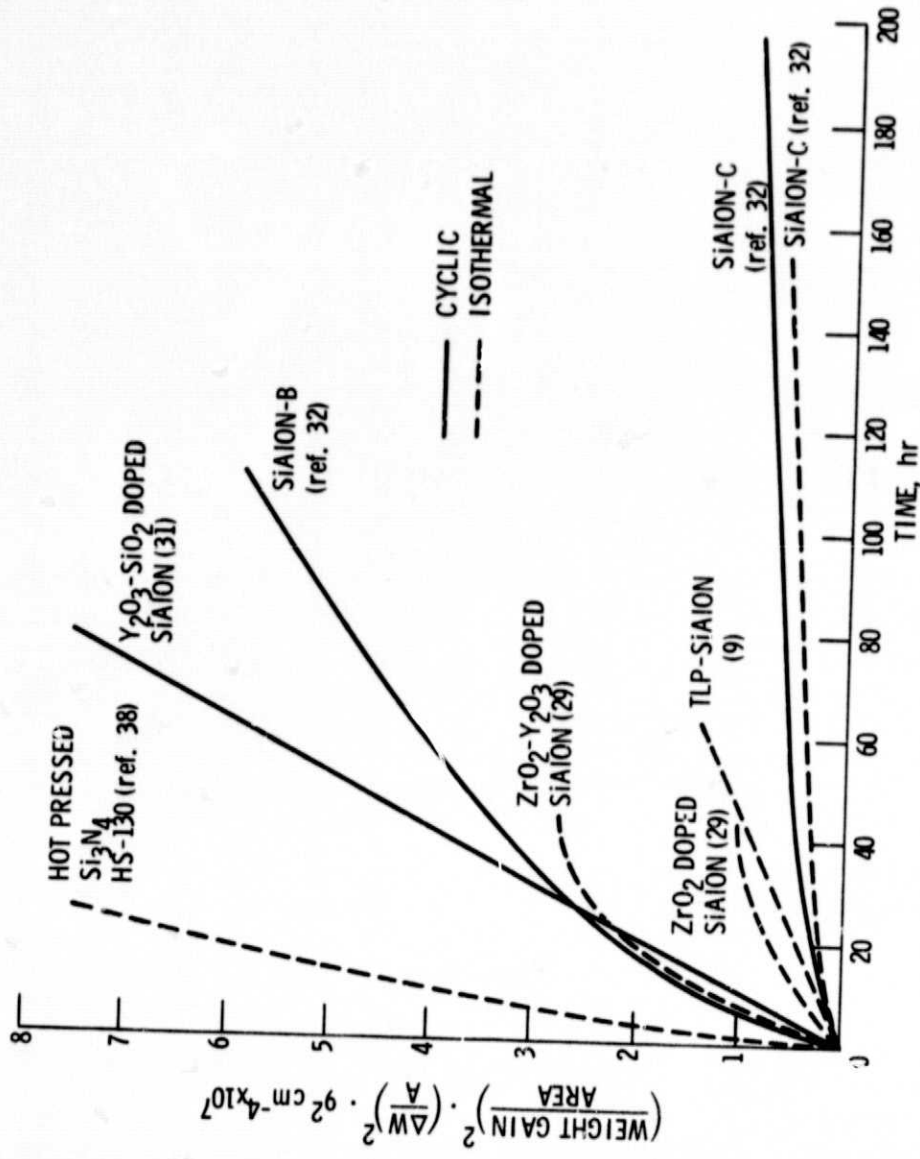


Figure 14. - Parabolic plots of the oxidation of various  $\text{Si}_3\text{N}_4$  ceramics at 1370° to 1400° C.

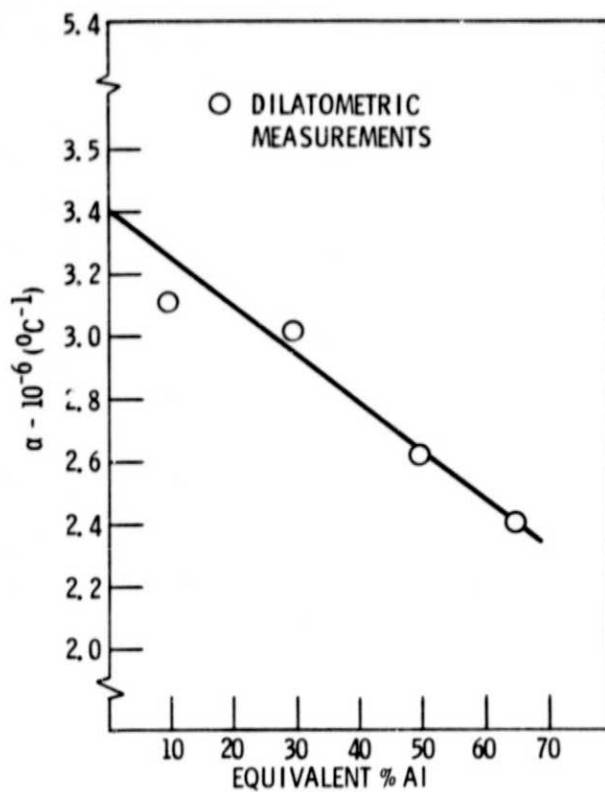


Figure 15. - Linear coefficient of thermal expansion between 25<sup>o</sup> and 1000<sup>o</sup> C for  $\beta'$  -  $\text{Si}_{6-x}\text{Al}_x\text{O}_x\text{N}_{8-x}$  SiAlON (after Gauckler, ref. 18).